

# Predictive Deployment of UAV Base Stations in Wireless Networks: Machine Learning Meets Contract Theory

Qianqian Zhang<sup>1</sup>, Walid Saad<sup>1</sup>, Mehdi Bennis<sup>2</sup>, Xing Lu<sup>3</sup>, Mérouane Debbah<sup>4,5</sup>,  
and Wangda Zuo<sup>3</sup>

<sup>1</sup>Bradley Department of Electrical and Computer Engineering, Virginia Tech, VA, USA, Emails: {qqz93,walids}@vt.edu

<sup>2</sup>Center for Wireless Communications-CWC, University of Oulu, Finland, Email: mehdi.bennis@oulu.fi

<sup>3</sup>Department of Civil, Environmental and Architectural Engineering, University of Colorado Boulder, CO, USA, Email: {xing.lu-1,wangda.zuo}@colorado.edu

<sup>4</sup>Mathematical and Algorithmic Sciences Lab, Huawei France R&D, Paris, France, Email: merouane.debbah@huawei.com

<sup>5</sup>Large Systems and Networks Group (LANEAS), CentraleSupélec, Université Paris-Saclay, Gif-sur-Yvette, France

## Abstract

In this paper, a novel framework that enables a predictive deployment of unmanned aerial vehicles (UAVs) as temporary flying base stations (BSs) to complement ground cellular systems in face of prospective steep surges in wireless traffic is proposed. Considering the downlink communications, the goal is to efficiently offload excessive wireless traffic from congested ground cellular networks (e.g. hotspot areas) to flying UAVs. In order to provide delay-free aerial service to such hotspot areas, first, a novel machine learning framework, based on wavelet decomposition and compressive sensing, is proposed to model the cellular traffic pattern, and predict the occurrence of traffic congestion. Given the predicted cellular traffic demand, a contract matching problem is then formulated to study the optimal allocation of UAVs to hotspot areas for traffic offloading. In order to employ a UAV with enough communication capacity at a reasonable price, a new approach based on contract theory is proposed that enables each BS to determine the payment charged to each employed UAV based on predicted demand while guaranteeing that each UAV truthfully reveals its communication capacity. To optimally allocate each UAV to hotspot areas, a matching approach is applied to jointly maximize the individual utility of each BS and UAV. The prediction error of the proposed machine learning framework is analytically derived and the results based on a real dataset show that the proposed approach yields a performance gain of 10% and 13% in overall prediction accuracy, and 28.3% and 56.6% improvement of the demand prediction during hotspot events, compared with the support vector machine and the weighted expectation maximization methods, respectively. Simulation results show that the proposed predictive deployment of UAVs can yield a two-fold improvement on average per BS utility and a 60% improvement on average per UAV utility, respectively, compared with a baseline, event-driven allocation of UAVs to ground hotspot areas.

A preliminary version of this work appears in the proceedings of IEEE GLOBECOM 2018 [1].

*Index Terms* – cellular networks; UAV deployment; traffic prediction; wavelet transform; compressive sensing; contract theory.

## I. INTRODUCTION

The use of unmanned aerial vehicles (UAVs) as flying base stations (BSs) has attracted growing interest in the past few years [1]–[7]. Flying UAV BSs can provide reliable uplink and downlink services for ground users and can potentially increase the network capacity, eliminate coverage holes of the existing cellular systems, and cope with the steep surge of communication needs in hotspot areas [1], [2]. Compared with the terrestrial BSs that are deployed at a fixed location for a long term, UAVs can rapidly change their positions to provide temporary on-demand service [3]. For instance, UAV BSs can be deployed to service major events (e.g. sport or musical events) during which the terrestrial network capacity is often strained, or to provide communication capabilities for disaster areas in which the ground cellular systems are damaged and cannot provide regular service [4]. Furthermore, UAVs can adjust their positions and establish line-of-sight (LOS) communication links towards ground users, thus improving network performance [5]. Due to the broad range of their application domains and their low cost, UAVs as flying BSs is a promising solution to provide temporary connectivity for ground users [6].

However, the deployment of UAVs to provide on-demand cellular service for hotspot areas faces several key challenges. For instance, flying UAV BSs are strictly constrained by their onboard energy, which should be efficiently used for communication. However, the on-demand deployment requires UAVs to continuously change their positions to meet instant communication requests. Therefore, most of their energy can be consumed by mobility, thus limiting their communication capabilities [1]. Furthermore, deploying UAVs to serve hotspot areas must be done a priori, in order to avoid unnecessary delays due to the travel time of the UAVs. In other words, a network operator must be able to predict, a priori, its hotspot or congestion events, so as to request UAV assistance ahead of time. These challenges, in turn, motivate the need for a comprehensive prediction of cellular traffic, and a predictive approach for UAV deployment [8]. To this end, machine learning (ML) techniques can be applied to analyze the pattern of the cellular traffic demand, thus forecasting the occurrence of traffic congestion, as well as estimating the supply-demand gap within the cellular networks. Given the predicted traffic demand, each BS can pinpoint congestion events and request assistance from UAVs if needed.

Another practical challenge of UAV deployment for aerial cellular service is to incentivize cooperation between the cellular network operator and the UAV operators. As shown in [9], UAV BSs and ground BSs will often belong to multiple operators, each selfishly seeking to maximize its individual benefit. To request a UAV's assistance, a ground BS needs to offer a reward to a UAV operator for the aerial wireless service. However, since the ground BS operator has no prior knowledge about the communication capacity of each UAV, the UAV operator can misrepresent the transmission capability of its UAV BSs to get a higher payment, or directly refuse the offloading request from a ground BS if the offered reward is too low. Therefore, to address this practical challenge, an incentive mechanism must be designed to promote cooperation among network operators, while guaranteeing truthful interactions between the operators of the ground and aerial networks.

#### *A. Related Works*

The optimal deployment of UAVs as aerial BSs has recently attracted significant attention [10]–[12]. In [10], the authors studied the optimal locations and coverage areas of aerial BSs under the objective of minimizing the transmit power. The work in [11] derived the minimum number of UAVs to satisfy the coverage and capacity constraints of the wireless system. In [12], the authors jointly optimized the UAV trajectory and the network resource allocation in order to maximize the throughput to ground users. The problem of traffic offloading from an existing wireless network via UAV BSs has been addressed in [13]–[16]. In [13], the allocation problem of UAVs to each geographic area was investigated to improve the spectral efficiency and reduce the delay. In [14] and [15], the authors optimized the trajectory of UAVs to provide wireless services to the cell-edge users. In [16], an unsupervised learning approach was presented to solve the 3D deployment of a fleet of UAVs for traffic offloading. However, most of the existing works [10]–[16] assumed that the traffic demand of the cellular users is known a priori, which is challenging to have in a practical network. Furthermore, the works [10]–[16] optimized the performance of the cellular network in a centralized approach which assumes all UAVs belong to the same entity. Given the fact that UAV BSs can belong to multiple operators, a new framework of UAV deployment is needed which considers the utility of the aerial UAVs in the traffic offloading, while optimizing the performance of cellular network.

Meanwhile, in [17]–[19], a number of ML approaches have been proposed to predict the data demands of cellular networks. In [17], a traffic prediction framework was proposed to model the

cellular data in the temporal domain and the spatial domain. In [18], the authors proposed an ML framework, based on pattern modeling, to predict the locations of mobile users during daily activities. The work [19] provided surveys that focused on the general use of ML algorithms in cellular networks. Furthermore, the prior art in [20]–[22] studied the use of ML techniques to improve the performance of UAV-aided communications. In [20], an ML framework based on liquid state machine is proposed to optimize the caching content of each UAV BS, as well as the resource allocation strategies. In [21], the authors investigated an ML approach to construct a radio map for autonomous path planning and positioning of UAVs. In [22], ML algorithms are applied to detect the presence of aerial users and distinguish them from the ground mobile users. However, most of the works in [17]–[22] aim to build an ML model to predict regular cellular traffic patterns, rather than focusing on identifying hotspot and network congestion events. In fact, none of the approaches proposed in [17]–[22] can effectively forecast the occurrence of network congestion events or accurately predict excessive traffic load in a cellular network during hotspot events. Therefore, the results of these prior works cannot be used to enable a predictive deployment of UAV networks for on-demand cellular service.

### *B. Contributions*

The main contribution of this paper is a novel framework for predictive on-demand deployment of UAV aerial BSs to alleviate congestion in hotspot areas of terrestrial cellular networks. In particular, we study a network in which UAVs are deployed as aerial BSs to complement the connectivity of a ground cellular system in face of a prospective surge in data demand. Our main contributions include:

- We jointly analyze the prediction of cellular traffic demand, and the deployment of UAVs to serve hotspot areas, by using a distributed approach. We assume that BSs and UAVs can belong to different operators each of which aiming to maximize its own individual utility (objective) function.
- A novel ML framework, based on wavelet decomposition and compressive sensing, is proposed to predict the traffic demand for each cellular system. In particular, the proposed approach can detect the cellular network congestion, model the traffic pattern of regular cellular communications, as well as predict the cellular data demand during hotspot events. To characterize the performance of the proposed ML framework, we analytically derive an upper bound on the prediction error. Compared to other ML methods such as weighted

expectation maximization (WEM) and support vector machines (SVMs), the proposed ML approach yields 10% and 13% gain in overall prediction accuracy, and 28.3% and 56.6% improvement on demand prediction during hotspot events, respectively.

- Given the predicted cellular traffic demand, a set of distributed optimization problems for each BS and each UAV operator is formulated to study the optimal allocation of UAVs to hotspot areas for cellular traffic offloading purposes. First, to employ a UAV with enough transmission power at a reasonable price, each BS designs a contract for each UAV that defines the service that the UAV needs to provide and the reward it will receive at the traffic offloading. We analytically derive the sufficient and necessary conditions of feasible contracts [23] that guarantee each UAV operator to truthfully reveal its communication capacity. Then, to find an optimal allocation of UAV BSs to each hotspot area, a matching approach is applied to jointly maximize the utility of each BS and UAV operator in a distributed approach. Simulation results show that the proposed predictive deployment of UAVs yield a two-fold improvement on average per BS utility and a 60% improvement on average per UAV utility, compared with a baseline, event-driven allocation of UAVs to ground hotspot areas.

The rest of this paper is organized as follows. In Section II, we present the system model and the problem formulation. In Section III, the ML approach is proposed to predict data demands. In Section IV-A, the traffic offload contract is designed between each BS and each UAV. To find the optimal allocation of UAVs, a matching framework is proposed in Section IV-B. Simulation results are presented in Section V. Finally, conclusions are drawn in Section VI.

## II. SYSTEM MODEL AND PROBLEM FORMULATION

Consider a set  $\mathcal{I}$  of  $I$  cellular BSs providing downlink wireless service to mobile users in a geographical area  $\mathcal{A}$ . Each BS  $i \in \mathcal{I}$  has a service area  $\mathcal{A}_i$ , such that  $\cup_{i \in \mathcal{I}} \mathcal{A}_i = \mathcal{A}$ , and  $\mathcal{A}_i \cap \mathcal{A}_k = \emptyset$  for any  $i \neq k$ , and  $i, k \in \mathcal{I}$ . In this network, a set  $\mathcal{J}$  of  $J$  flying UAVs that belongs to different operators from the ground cellular network can be used by the ground network as aerial BSs to provide additional aerial cellular service to the mobile users, particularly during hotspot events. We assume that each mobile user equipment (UE) can receive data from both the ground BSs and flying UAVs. Initially, a given UE will connect to one of the ground BSs. However, as shown in Fig. 1, if a ground BS is highly loaded, the BS can request assistance from an aerial UAV BS, and offload the service of some UEs to this UAV. Hereinafter, we use



Fig. 1: The red BSs are having excessive traffic load in the downlink, thus each red BS requests a UAV to offload a part of UEs to the aerial cellular system.

the term *UAV users* to indicate UEs that are served by aerial BSs. For tractability, we assume that, at each time, each BS can employ only one UAV for aerial cellular service, and each UAV only serves the area of a single BS. We also assume that different frequency bands are employed for the ground BS and UAV downlink communications. Moreover, as done in [24], each UAV is equipped with a directional antenna array that uses beamforming to transmit data to its users in the downlink. Therefore, interference between UAV transmissions is negligible.

#### A. Air-to-ground channel model

The path loss of the air-to-ground communication link from a typical UAV located at  $\mathbf{x} \in \mathbb{R}^3$  to a typical ground user that is located at  $\mathbf{y} \in \mathbb{R}^3$  can be given by [25]:

$$h[dB](\mathbf{x}, \mathbf{y}) = 20 \log \left( \frac{4\pi f_c \|\mathbf{x} - \mathbf{y}\|}{c} \right) + \xi(\mathbf{x}, \mathbf{y}), \quad (1)$$

where  $f_c$  is the carrier frequency of UAV downlink communications,  $\|\mathbf{x} - \mathbf{y}\|$  is the distance between the UAV and the UE,  $c$  is the speed of light, and  $\xi(\mathbf{x}, \mathbf{y})$  is the excessive path loss of the air-to-ground channel, which is an additional component to the free space propagation loss. Here, we assume that before offloading the service, the BS will estimate the channel state between the wireless users with the target UAV. As a result, each UAV user has an LOS link with the associated UAV. Therefore, the additional path loss can be modeled using a Gaussian distribution  $\xi(\mathbf{x}, \mathbf{y}) \sim \mathcal{N}(\mu_{\text{LOS}}, \sigma_{\text{LOS}}^2)$  [25].

Consequently, the achievable data rate that a UAV  $j \in \mathcal{J}$  located at  $\mathbf{x}_j$  can provide to a UE at  $\mathbf{y} \in \mathcal{A}_i$  in the service area of BS  $i$  can be given by:

$$r_{ij}(\mathbf{x}_j, \mathbf{y}) = w \log_2 \left( 1 + \frac{g(\mathbf{x}_j, \mathbf{y}) p_j}{h(\mathbf{x}_j, \mathbf{y}) w n_0} \right), \quad (2)$$

where  $w$  is the bandwidth of each UAV downlink link,  $g(\mathbf{x}_j, \mathbf{y})$  is the antenna gain of UAV  $j$  towards the UE located at  $\mathbf{y}$ ,  $p_j$  is the transmit power of UAV  $j$ ,  $h(\mathbf{x}_j, \mathbf{y})$  is the path loss in linear scale, and  $n_0$  is the average noise power spectrum density at the UE. Here, we consider a perfect beam alignment between each UAV BS and its served UEs, and we assume that each UAV has the same maximum antenna gain [26]. Therefore,  $g(\mathbf{x}_j, \mathbf{y}) = g$ , which is a constant for all  $j \in \mathcal{J}$ ,  $\mathbf{x}_j \in \mathcal{A}$ , and  $\mathbf{y} \in \mathcal{A}_i$ . Let  $f_i(\mathbf{y})$  (with  $\mathbf{y} \in \mathcal{A}_i$ ) be the spatial distribution of UAV users that BS  $i$  offloads to the requested UAV, where  $\int_{\mathcal{A}_i} f_i(\mathbf{y}) d\mathbf{y} = 1$ . Then, the average capacity that UAV  $j$  can provide to the UAV users from the service area of BS  $i$  will be

$$\begin{aligned} r_{ij}(\mathbf{x}_j, p_j) &= \int_{\mathcal{A}_i} r_{ij}(\mathbf{x}_j, \mathbf{y}) f_i(\mathbf{y}) d\mathbf{y}, \\ &= \int_{\mathcal{A}_i} w \log_2 \left( 1 + \frac{gp_j}{h(\mathbf{x}_j, \mathbf{y})wn_0} \right) f_i(\mathbf{y}) d\mathbf{y}. \end{aligned} \quad (3)$$

Note that, in (3), the variables are the location  $\mathbf{x}_j$  of UAV  $j$  and its transmit power  $p_j$ . Here, following from [10], we assume that the location  $\mathbf{x}_{ij}^*$  of the target UAV has been optimized, based on the UAV user distribution  $f_i(\mathbf{y})$  and the service area  $\mathcal{A}_i$  of BS  $i$ . Therefore, the downlink transmission  $p_j$  is the only variable that UAV  $j$  can still control to optimize the average capacity  $r_{ij}(p_j)$ . Furthermore, in order to simplify the analysis, we assume that each UAV serves the UEs associated with a given BS for a constant interval  $T$ . Then, by serving the UAV users from BS  $i$  for a period of  $T$ , the average amount of data that UAV  $j$  can provide will be

$$B_{ij}(p_j) = T \cdot r_{ij}(p_j). \quad (4)$$

### B. Data Demand of cellular networks

Given the amount of data  $B_{ij}(p_j)$  that each UAV  $j \in \mathcal{J}$  can provide during each period  $T$ , each BS  $i \in \mathcal{I}$  should know if this communication capacity of UAV  $j$  is enough to satisfy its traffic demand. Thus, the next task for each BS is to estimate the data demand in its cellular network and identify possible congestion events. On the one hand, once the predicted traffic demand exceeds the network capacity, each BS can request the assistance of a UAV to offload some users to the aerial BS beforehand, and therefore, alleviate future network congestion events. On the other hand, the predicted traffic demand enables each BS to find a suitable UAV that has enough power to fill the supply-demand gap within its cellular system. These requirements, in turn, motivate a *predictive* approach to UAV deployment. To this end, each BS  $i \in \mathcal{I}$  must use ML techniques to predict the downlink cellular traffic. Let  $\tilde{d}_i(t)$  be the predicted supply-demand

gap between the downlink capacity of BS  $i$  with the data demand of cellular users within  $\mathcal{A}_i$ , from time  $t$  to time  $t + T$ . Naturally, once  $\tilde{d}_i(t) > 0$ , BS  $i$  should request a UAV  $j \in \mathcal{J}$  with enough power  $p_j$  to offload part of cellular service, such that  $B_{ij}(p_j) \geq \tilde{d}_i(t)$ .

In order to perform the ML-based prediction of data demand, each BS  $i \in \mathcal{I}$  can exploit a dataset of the cellular traffic history. The dataset can be represented by a vector  $\mathbf{d}_i = [d_i(t) \mid \forall t \in \mathcal{T}]$ , where  $\mathcal{T} = \{T, 2T, \dots, MT\}$  is a discrete time set of the past, and  $d_i(t)$  is the amount of downlink data service that BS  $i$  offloads to a UAV during a time interval from  $t$  to  $t + T$ . Therefore, at the beginning of each period  $t$ , each BS  $i$  estimates the aerial data demand  $\tilde{d}_i(t)$  for the next time interval from  $t$  to  $t + T$ , and requests a UAV BS for assistance if needed, according to the prediction result.

### C. Utility function for a ground BS

Given the predicted data demand  $\tilde{d}_i(t)$  of UAV users from each BS  $i$  and the downlink capacity  $B_{ij}(p_j)$  of each UAV  $j$ , the next step is to allocate UAVs to each BS that is in need for assistance. Here, we first define utility function for the BS. Each BS  $i \in \mathcal{I}$  will employ a UAV  $j \in \mathcal{J}$  to offload its service for a time period  $T$  while maximizing the following utility function:

$$U_{ij}(u_i, p_j, \tilde{d}_i(t)) = \beta B_{ij}(p_j) - u_i \tilde{d}_i(t) - \delta \|\tilde{d}_i(t) - d_i(t)\|, \quad (5)$$

where  $\beta$  is the payment per bit of data that mobile users give to BS  $i$  for data service,  $B_{ij}(p_j)$  is the data amount that UAV  $j$  will provide to the UEs of BS  $i$ ,  $u_i$  is the unit payment that BS  $i$  gives to UAV  $j$  per bit of data service,  $\tilde{d}_i(t)$  is the predicted demand of aerial data traffic within  $\mathcal{A}_i$ ,  $d_i(t)$  is the actual data demand, and  $\delta > u_i$  is a loss parameter of the prediction error  $\|\tilde{d}_i(t) - d_i(t)\|$ . Therefore, the first term in (5) represents the reward that BS  $i$  gets from its UEs by employing UAV  $j$  to provide the aerial downlink service, the second term in (5) is the total payment that BS  $i$  gives to UAV  $j$ , based on its predicted data demand  $\tilde{d}_i(t)$ , and the third term in (5) is the penalty for inaccurate prediction of cellular data demand. Consequently, the utility in (5) represents the total income of BS  $i$  by employing UAV  $j$  for aerial cellular service.

Due to the imperfection of ML-based prediction, the estimated traffic amount  $\tilde{d}_i(t)$  can be different from the actual data demand  $d_i(t)$ . However, when the predicted demand  $\tilde{d}_i(t)$  is lower than the actual data demand  $d_i(t)$ , the predictive deployment of UAVs will not prevent the occurrence of network congestion. On the other hand, if the predicted data demand  $\tilde{d}_i(t)$  is higher than the actual need  $d_i(t)$ , no network congestion will happen. However, BS  $i$  will have to pay

more to UAV  $j$  for its aerial cellular service, which in turns lowers the utility of BS  $i$ . Therefore, the maximum value of (5) can be achieved with a perfect prediction, where  $\tilde{d}_i(t) = d_i(t)$ .

Note that, the data amount  $B_{ij}(p_j)$  that UAV  $j$  actually provides to the users of BS  $i$  can be different from the predicted traffic amount  $\tilde{d}_i(t)$  or the real demand  $d_i(t)$ . Since UAV  $j$  controls the value of  $p_j$  which is not revealed to BS  $i$ , UAV  $j$  can misrepresent its available transmit power, when each BS requests for aerial service at the beginning of each interval. To avoid scenarios in which UAV operators misrepresent their communications capabilities to get higher rewards, each BS needs to design the value of the unit payment  $u_i$  carefully, based on the transmit power  $p_j$  of UAV  $j$ , as explained in Section IV.

#### D. Energy model and utility function for a UAV

UAV power consumption is generally composed of two components: the aforementioned transmit power  $p_j$ , and the power  $p_j^m$  used for mobility and propulsion. Generally, the propulsion power  $p_j^m$  takes a great majority of the total power consumption. If UAV  $j$  travels from its current location  $\mathbf{x}_j$  to the optimal service location  $\mathbf{x}_{ij}^*$  of a typical BS  $i$ , the amount of mobility energy consumed during this travel will be  $e_{ij}(p_j^m) = p_j^m \cdot \frac{\|\mathbf{x}_j - \mathbf{x}_{ij}^*\|}{v(p_j^m)}$ , where  $\|\mathbf{x}_j - \mathbf{x}_{ij}^*\|$  is the displacement distance, and  $v(p_j^m)$  is the average speed of UAV  $j$  which depends on the propulsion power  $p_j^m$ . The optimal mobility power  $p_j^{m*} = \arg \min_{p_j^m} e_{ij}$  that minimizes UAV energy consumption on the travel has been derived in [27, (6) to (8)]. Let  $E_j$  be the onboard energy of UAV  $j$  before travel. Then, after flying from  $\mathbf{x}_j$  to  $\mathbf{x}_{ij}^*$ , the remaining onboard energy of UAV  $j$  is  $E_j - e_{ij}(p_j^{m*})$ . Thus, the maximum available power that UAV  $j$  can use for wireless communications will be  $p_{ij}^{\max} = \frac{E_j - e_{ij}(p_j^{m*})}{T}$ . Therefore, the value of transmit power  $p_j$  can range within  $[0, p_{ij}^{\max}]$ .

Consequently, for each UAV  $j \in \mathcal{J}$ , the utility achieved from providing aerial cellular service to UAV users of BS  $i$  is given by

$$R_{ij}(u_i, p_j, \tilde{d}_i(t)) = u_i \tilde{d}_i(t) - T c_{ij} p_j, \quad (6)$$

where  $c_{ij}$  is the unit cost of communication power that UAV  $j$  provides to UEs of BS  $i$  in the downlink. The first term in (6) is the reward that UAV  $j$  gets from serving BS  $i$ , and the second term in (6) is the cost for providing downlink communication service with a transmit power  $p_j$ . Thus, the utility in (6) is the total income of UAV  $j$  by serving BS  $i$  for a period time  $T$ .

Note that, the value of the unit cost  $c_{ij}$  depends on the maximum transmit power  $p_{ij}^{\max}$ . Here, we model the relationship between  $c_{ij}$  and  $p_{ij}^{\max}$  by an inverse proportional function as  $c_{ij} = \frac{\alpha_j}{p_{ij}^{\max}}$ , where  $\alpha_j$  is a positive constant. It shows that if UAV  $j$  has enough communication power  $p_{ij}^{\max}$ , it will provide aerial service to BS  $i$  at a low price. However, if the available communication  $p_{ij}^{\max}$  power is very limited, a higher price  $c_{ij}$  will be charged.

### E. Problem formulation

By comparing (5) and (6), we can see that  $\arg \max_{u_i, p_j} U_{ij} = \arg \min_{u_i, p_j} R_{ij}$ , and, thus, the BS and the UAV operators have conflicting interests. Note that, ground BSs and UAVs belong to different operators, and each aims to maximize its individual utility. In order to resolve the conflict, each BS  $i \in \mathcal{I}$  should carefully design the value of payment  $u_i$ , according to the transmit power  $p_j$ , such that the values of  $(u_i, p_j)$  are beneficial for both the ground and aerial network operators. Meanwhile, to prevent the UAVs from misreporting their communication capacity, an incentive mechanism is needed to guarantee truthful interactions between the BS and UAV operators. Here, we let  $\phi_{ij} = (u_i, p_j)$  be a *traffic offload contract* between BS  $i$  and UAV  $j$ , which defines the transmission power  $p_j$  that UAV  $j$  needs to provide and the reward  $u_i$  that BS  $i$  pays to UAV  $j$  for its traffic offloading service. The set of all possible contract  $\phi_{ij}$  between BS  $i$  with any UAV  $j$  is given by  $\Phi_i = \{\phi_{ij} | \forall j \in \mathcal{J}\}$ .

Consequently, each BS  $i \in \mathcal{I}$  aims to maximize its utility in (5) by predicting the data demand  $\tilde{d}_i(t)$  within its service area  $\mathcal{A}_i$ , designing the contract set  $\Phi_i$  for each UAV  $j \in \mathcal{J}$ , based on the predicted cellular traffic, and finally employing the optimal UAV  $j \in \mathcal{J}$  to offload service. We formulate this predictive UAV deployment problem as follows,

$$\max_{j \in \mathcal{J}, \Phi_i, \tilde{d}_i(t)} U_{ij}(\phi_{ij}, \tilde{d}_i(t)), \quad (7a)$$

$$\text{s. t. } p_j \geq 0, \forall j \in \mathcal{J}, \quad (7b)$$

$$0 \leq u_i \leq \delta, \forall i \in \mathcal{I}, \quad (7c)$$

$$\tilde{d}_i(t) \geq 0. \quad (7d)$$

The objective function (7a) is the utility of each BS  $i$  when employing a UAV  $j$ . (7b) ensures that the transmit power is non-negative. (7c) and (7d) are constraints of ML-based prediction. Note that, the prediction of data demand  $\tilde{d}_i(t)$  and the design of the traffic offloading contract  $\Phi_i$  are determined only by BS  $i$  itself, and, thus, they can be locally optimized. However, the

solution of problem (7) not only determines the utility of BS  $i$ , but also decides the utility of a UAV, while at the same time, each UAV  $j \in \mathcal{J}$  aims to choose the optimal BS  $i \in \mathcal{I}$  that maximizes its individual utility, given as follows:

$$\max_{i \in \mathcal{I}} R_{ij}(\phi_{ij}), \quad (8a)$$

$$\text{s. t. } 0 \leq p_j \leq p_{ij}^{\max}, \forall j \in \mathcal{J}. \quad (8b)$$

The objective function (8a) is the utility of UAV  $j$  when serving BS  $i$ . (8b) is the constraint of the maximal available transmission power of UAV  $j$ . Thus, the optimization problems (7) and (8) are interdependent with each other, and must be solved jointly.

However, jointly solving problems (7) and (8) is challenging. First, since ground BSs and UAVs belong to different operators, each aims to maximize its individual utility, and, thus, a distributed approach needs to be developed. However, due to the interdependency of the utilities of each BS and UAV, one solution of (7) determines the output of problem (8), and vice versa. Thus, the classical distributed optimization approaches [28] cannot be applied directly to solve the problems. Furthermore, given that, at each time, each BS can employ only one UAV for aerial cellular service and each UAV only serves the area of a single BS, the solution of each BS  $i$  in problem (7) not only depend on the utility that BS  $i$  can provide to the selected UAV, but is also determined by the utilities that other BSs offer to the UAV. To properly model the interactions between BSs and UAVs and jointly optimize the utility of each operator in a distributed approach, we use two key frameworks: contract theory [23], to induce truthfulness and matching theory [29], to devise tractable distributed solutions for the optimization problems in (7) and (8), while accounting for the contract-theoretic constraints. Therefore, in Section IV-B a matching approach will be explored to solve problems (7) and (8).

Consequently, to solve the predictive deployment problem of aerial UAV BSs, we will first propose an ML-based approach that enables the prediction of aerial traffic demand  $\tilde{d}_i(t)$  for each BS  $i \in \mathcal{I}$  in Section III, then in Section IV-A, the traffic loading contract  $\Phi_i$  is designed, based on the predicted data demand. Finally, a matching-theoretic solution is developed to derive the optimal UAV-BS allocation.

### III. ML-BASED PREDICTION OF CELLULAR TRAFFIC DEMAND

In order to maximize the objective function in (7) for each BS  $i \in \mathcal{I}$ , the prediction of data demand  $\tilde{d}_i(t)$  should be estimated so as to approximate, as accurately as possible, the real

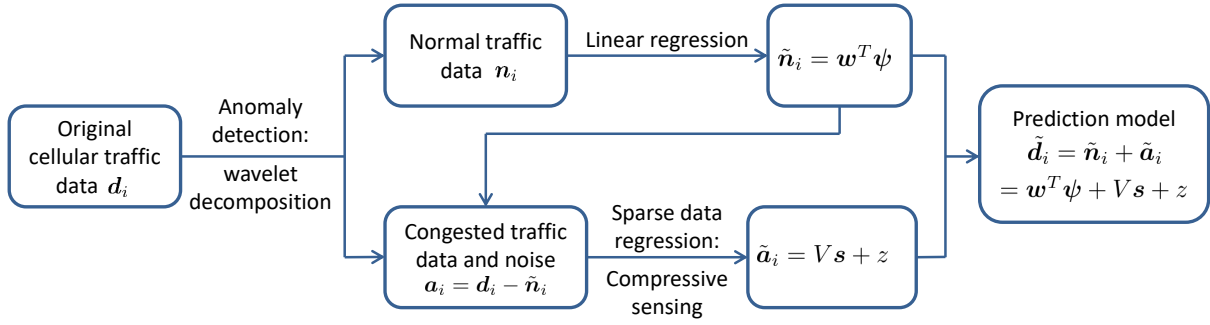


Fig. 2: The proposed traffic demand prediction framework.

traffic need  $d_i(t)$ . To this end, we propose a novel ML-based framework to model the pattern of cellular traffic, thus enabling the prediction of the traffic demand and the occurrence of network congestion. For each BS  $i \in \mathcal{I}$ , the past traffic history is given as  $\mathbf{d}_i = [d_i(t) \mid \forall t \in \mathcal{T}]$ , where  $\mathcal{T} = \{T, 2T, \dots, MT\}$  is a discrete set of time (e.g., in hours), and  $d_i(t)$  is the amount of downlink data that BS  $i$  offloads to a UAV during a time interval from  $t$  to  $t + T$ . The network needs to predict the traffic volume  $\tilde{d}_i(t)$  for a future moment  $t$ , given the time-series dataset  $\mathbf{d}_i$ .

Fig. 2 illustrates the proposed ML-based cellular traffic prediction framework. Given the traffic data  $\mathbf{d}_i$ , each BS  $i \in \mathcal{I}$  first distinguishes the normal cellular traffic from anomalous traffic, using wavelet decompositions. Here, anomalous traffic pertains to a high-volume traffic load, which, in turn, indicates the occurrence of network congestion. Then, two regression approaches will be used to model the regular and the anomalous cellular traffic data, respectively. For the regular traffic load  $\mathbf{n}_i$ , since the data presents a repetitive daily pattern, which is easy to track, a traditional linear regression approach will be applied to build a noise-free model  $\tilde{\mathbf{n}}_i$ . Based on the normal traffic model  $\tilde{\mathbf{n}}_i$ , the dataset of congested cellular traffic load with noise is obtained by  $\mathbf{a}_i = \mathbf{d}_i - \tilde{\mathbf{n}}_i$ . Different from previous works [17]–[22] that take  $\mathbf{a}_i$  as outliers and ignore them in their models, we propose a compressive time-dependent model, which enables traffic prediction even during cellular congestion or hotspot events. In this regard, to model the pattern of network congestion, a sparse data regression technique, based on compressive sensing, is applied to identify the reasons that cause the network congestion in the downlink, and find the relationship between congestion reasons with the excess amount of cellular traffic load during the congestion events. Here, a database of City Cellular Traffic Map [30] will be used to illustrate the modeling process and evaluate the performance of the proposed ML framework. Without loss of generality, our approach can accommodate other datasets. To our best knowledge, this is the first work to model the cellular traffic load for both a regular pattern and network congestion

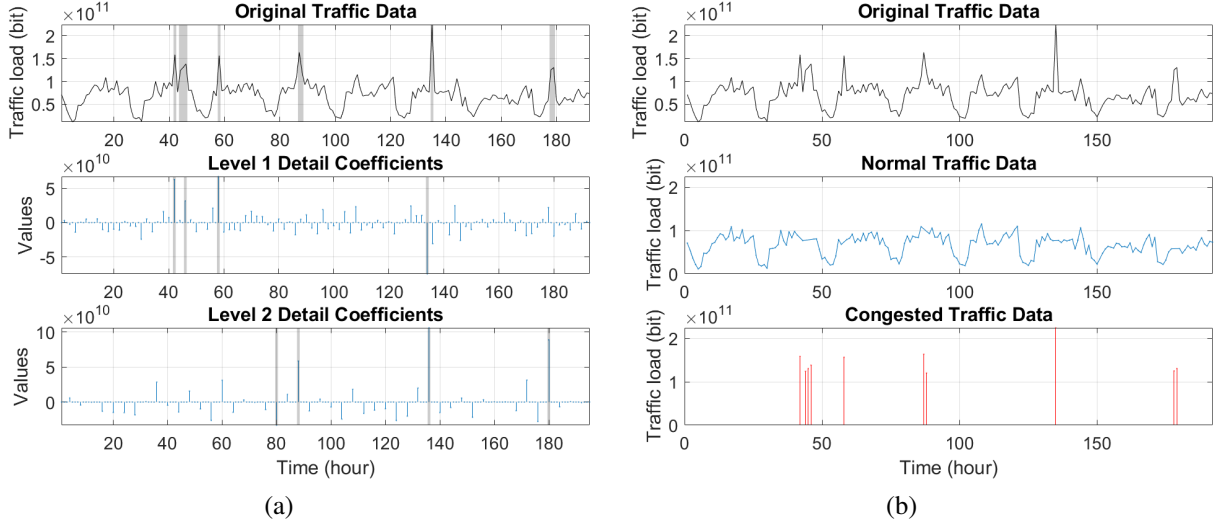


Fig. 3: (a) Two-level DWT is applied to detect the sudden surge of the cellular traffic load. (b) The dataset  $d_i$  will be divided, according to the DWT result, into two subsets, which are the normal traffic load  $n_i$  (the middle figure) and the potential congested cellular data (the bottom figure).

events.

#### A. Detection of congestion events

As shown in Fig. 3, the original cellular traffic presents a conspicuously periodic pattern, with several sudden and erratic surges. In order to model the traffic pattern comprehensively, first, we develop an anomaly detection scheme based on the discrete wavelet transform (DWT) [17] in order to separate the normal cellular traffic load from the anomalous data.

DWT is a powerful technique to process data that exhibits a regular structure, such as successive time points in a temporal sequence, or pixels in an image. It has been widely applied to explore the transient abnormal phenomenon from normal signals and demonstrate its components [31]. DWT considers basis functions that are localized in both space and frequency domains. Specifically, DWT can decompose a time series into multi-level components based on a variant of frequencies, in which the lower-frequency component defines the long term trend of the data, whereas the higher-frequency component represents the small-scale rapid signal variation [32]. Note that traffic congestion in a cellular network usually exhibits a steep surge in the traffic load, thus causing a sudden change in the frequency domain. Consequently, DWT can properly detect cellular traffic congestion in  $d_i$  by capturing this frequency change.

The steep surge of the traffic load in  $d_i$  can be captured by the detail coefficients of higher-frequency component of DWT, given by [33]  $q_{j,t} = \sum_{l=1}^L g_l d_i(2t - l + 2 \bmod 2^j)$ , where  $j \in \{1, \dots, J\}$  is the decomposition level of DWT,  $L$  is the length of filter, and  $g_l$  is the  $l$ -th

component of the wavelet filter  $G$ . Fig. 3a shows the decomposition result of a two-level DWT with  $J = 2$ . The middle figure in Fig. 3a shows the detail coefficient  $q_{1,t}$  of the first-layer DWT, and the bottom figure shows the second-layer coefficient  $q_{2,t}$ .

Then, a hard thresholding is applied at each decomposition level  $j$  to detect congestion events, using the universal threshold (UT) [34] defined as,  $\tau_j = \frac{\text{median}(q_{j,t})}{0.6745} \sqrt{2 \log(M)}$ , where  $M$  is the number of data points in  $\mathbf{d}_i$ . If the absolute value  $|q_{j,t}|$  exceeds the threshold  $\tau_j$ , the data point will be regarded as an anomaly, i.e., a congestion event. Consequently, in Fig. 3a, the detected anomalies are marked in gray, and Fig. 3b shows the normal traffic load  $\mathbf{n}_i$  of each BS  $i$  which is obtained by filtering out the anomalies in  $\mathbf{d}_i$ , according to the detection result of DWT.

### B. Linear regression for normal traffic data

Linear regression is a well-developed technique that can be used to predict the data demand, by taking linear combinations of a fixed set of functions of time  $t$ . Due to the periodicity of human activity, cellular traffic  $\mathbf{n}_i$  often exhibits a repetitive daily pattern [35], which is easy to track. Based on this observation, we will use a linear regression model to model the normal traffic load curve for each single day, which is given by,

$$n_i(t) = \tilde{n}_i(t) + \epsilon, \quad (9)$$

where  $t \in \{T, 2T, \dots, NT\}$  with  $NT = 24$ ,  $n_i(t)$  is the actual traffic load of BS  $i$  from  $t$  to  $t + T$ , and no traffic congestion happens during each period,  $\epsilon$  denotes the noise that is modeled by a zero mean Gaussian random variable with variance  $\sigma_\epsilon^2$ , and  $\tilde{n}_i(t)$  is the proposed linear regression model, defined by  $\tilde{n}_i(t) = \mathbf{w}^T \boldsymbol{\psi}(t) = \sum_{s=1}^S w_s \psi_s(t)$ , where  $S$  is the number of basis functions in the linear regression model,  $\mathbf{w} = [w_1, \dots, w_S]^T$  is the parameter vector for linear combination, and  $\boldsymbol{\psi} = [\psi_1, \dots, \psi_S]^T$  is the vector of basis functions, with each  $\psi_s$  being a Gaussian function with mean  $t_s$  and variance  $\sigma_s^2$ . The values of parameters  $\{(t_s, \sigma_s^2) | s = 1, \dots, S\}$  can be determined by the weighted expectation maximization (WEM) algorithm, that we developed in [1], and the parameter  $\mathbf{w}$  is optimized by minimizing the sum-of-squares error with regularization term as follows [36]

$$\min_{\mathbf{w}} \sum_{n=1}^N [n_i(t_n) - \mathbf{w}^T \boldsymbol{\psi}(t_n)]^2 + \lambda \mathbf{w}^T \mathbf{w}, \quad (10)$$

where  $\lambda$  is the regularization coefficient. The optimization problem admits a closed-form solution  $\mathbf{w}^* = (\lambda \mathbf{I} + \Psi^T \Psi)^{-1} \Psi^T \mathbf{n}_i(\mathbf{t})$ , where  $\Psi = [\psi_1(\mathbf{t}), \dots, \psi_S(\mathbf{t})] \in \mathbb{R}^{N \times S}$ . Thus, the linear regression model of normal traffic data is given by  $\tilde{n}_i = \mathbf{w}^* \boldsymbol{\psi}(t)$ .

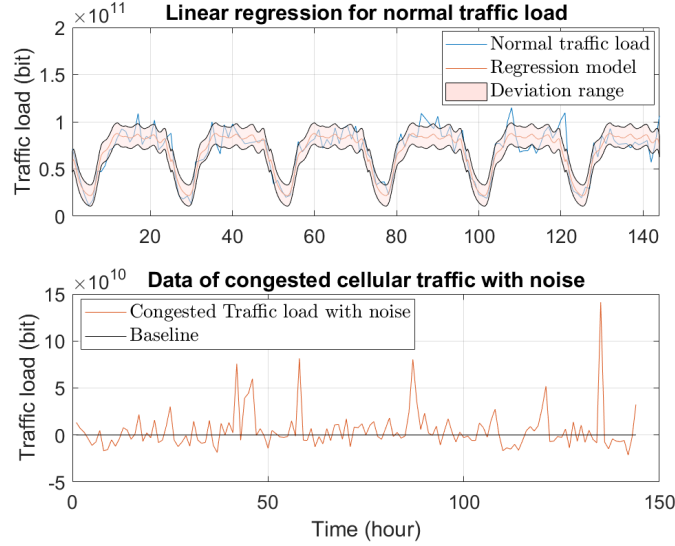


Fig. 4: The linear regression model of normal traffic load, and the dataset of congested cellular traffic.

By subtracting  $\tilde{n}_i$  from the original traffic data  $d_i$ , the dataset of congested traffic load with noise is obtained as  $a_i = d_i - \tilde{n}_i$ . The upper figure in Fig. 4 shows the linear regression model  $\tilde{n}_i$  for the normal traffic load, and the bottom figure illustrates the dataset  $a_i$ . The next step is to model the network congestion patterns, and predict the traffic amount during hotspot events.

### C. Sparse data regression for congested traffic data with noise

As shown in Fig. 4,  $a_i$  is composed of several steep surges in the cellular traffic load, with a perpetual disturbance near the baseline. Here, we model the small disturbance as an additive white Gaussian noise, and the pattern of traffic congestion will be explored via compressive sensing techniques. Compressive sensing techniques study the problem of sparse signal recovery [17] with the following typical form:

$$\tilde{a}_i(t) = \mathbf{V}(t)\mathbf{r}(t) + z, \quad (11)$$

where  $\mathbf{r}(t) \in \mathbb{R}^{H \times 1}$  is a sparse vector, which has  $K(t) \ll H$  non-zero components,  $\mathbf{V}(t) \in \mathbb{R}^{1 \times H}$  is the  $t$ -th row of the design matrix  $\mathbf{V}$ , and  $z$  represents the additive Gaussian noise with zero mean. In this cellular traffic prediction framework,  $\mathbf{r}(t)$  is called a reason vector, which represents the possible reasons in the service area of BS  $i$  that caused cellular traffic congestion in the downlink at time  $t$ , while the design matrix  $\mathbf{V}(t)$  defines the relationship between each congestion reason with the excess traffic amount during the hotspot event.

The model in (11) assumes that there is a total of  $H$  possible reasons that can cause a hotspot event in the cellular network of BS  $i$ , due to either an increase on the number of mobile users or

an increase in the data demand for each individual user. For example, a stadium located in the service area of BS  $i$  holds a football game every weekend. Due to the crowd of audience, BS  $i$  can experience a cellular traffic congestion during each game. Thus, the occurrence of each reason is highly time-related and can be periodic over a long term. However, for a specific load surge at time  $t$ , the number  $K(t)$  of active causes is much smaller, compared with the number of all possible reasons  $H$ . Consequently, the reason vector  $\mathbf{r}(t)$  in the compressive sensing model is defined as a time-dependent sparse vector.

In order to find the exact reasons that causes a load surge, the number  $K(t)$  of active reasons and the locations of the  $K(t)$  non-zeros in the vector  $\mathbf{r}(t)$  need to be explored. Moreover, the design matrix  $\mathbf{V}$ , which defines how the congestion reasons result in the demand surge, also needs further study. To find the best match of the compressive sensing model to the dataset  $\mathbf{a}_i$ , the following optimization problem is proposed,

$$\min_{\mathbf{V}, \mathbf{r}, z} \|\mathbf{a}_i - \tilde{\mathbf{a}}_i\|_2^2 + \lambda_1 \|z\|_2^2 + \lambda_2 \|\mathbf{r}\|_1, \quad (12)$$

where  $\|\mathbf{x}\|_p = (\sum x^p)^{\frac{1}{p}}$  is the  $\ell_p$ -norm of a vector. The first term in (12) represents the Euclidean distance of error between the compressive sensing model  $\tilde{\mathbf{a}}_i$  with the dataset  $\mathbf{a}_i$ . The second term guarantees that the noise power plays no dominant role during a traffic load surge. The third term is the  $\ell_1$ -norm of the reason vector  $\mathbf{r}$ , which is a relaxed constraint based on the  $\ell_0$ -norm of  $\mathbf{r}$  in the original compressive sensing problem, and it requires  $\mathbf{r}$  to be a sparse vector. The parameters  $\lambda_1 \geq 0$  and  $\lambda_2 \geq 0$  control the relative importance of the noise parameter and sparseness term, with respect to the Euclidean error, respectively [37].

In order to solve (12), a novel and iterative algorithm, based on a modified approach of the alternating direction method (ADM), is proposed in Algorithm 1, where (12) is optimized iteratively over  $\mathbf{V}$ ,  $\mathbf{r}$ , and  $z$ , respectively. In Algorithm 1, we first randomly initialize the design matrix  $\mathbf{V}$ , and then, apply the LASSO algorithm [38] to obtain the best-correlated sparse vector  $\mathbf{r}$  with respect to the current design matrix  $\mathbf{V}$ . Next, two auxiliary variables  $A$  and  $B$  are calculated, and the optimal design matrix  $\mathbf{V}$  is computed, via a dictionary update algorithm [39]. In the end of each iteration, the value of the noise term  $z$  is calculated by convex optimization to further minimize the value of the optimization function in (12). In summary, the proposed algorithm minimizes the error of ML prediction of traffic demand under congested network conditions, while considering the effect of noise.

---

**Algorithm 1** Proposed algorithm to determine the design matrix  $\mathbf{V}$ , the sparse vector  $\mathbf{r}$ , and the noise term  $z$

---

**Input:** the dataset  $\mathbf{a}_i$

**Initialization:** the design matrix  $\mathbf{V}^{(0)} \in \mathbb{R}^{M \times H}$ , the number of iterations  $J$ , two auxiliary matrices  $\mathbf{A}^{(0)} \in \mathbb{R}^{H \times H}$  and  $\mathbf{B}^{(0)} \in \mathbb{R}^{m \times H}$  with all zero elements, the noise term  $z^{(0)} \sim \mathcal{N}(0, 1)$ .

**For**  $j = 1$  to  $J$  **do**

1. Compute  $\mathbf{r}^{(j)}$  via LASSO algorithm [38] to obtain  $\mathbf{r}^{(j)} = \arg \min_{\mathbf{r}} \|\mathbf{a}_i - \mathbf{V}^{(j-1)} \mathbf{r} - z\|_2^2 + \lambda_2 \|\mathbf{r}\|_1$ .
2. Compute  $\mathbf{A}^{(j)}$  and  $\mathbf{B}^{(j)}$  via  $\mathbf{A}^{(j)} = \mathbf{A}^{(j-1)} + \mathbf{r}^{(j)}(\mathbf{r}^{(j)})^T$ ,  $\mathbf{B}^{(j)} = \mathbf{B}^{(j-1)} + \mathbf{a}_i(\mathbf{r}^{(j)})^T$ .
3. Compute  $\mathbf{V}^{(j)}$  via dictionary update algorithm [39, Algorithm 2] to obtain

$$\mathbf{V}^{(j)} = \arg \min_{\mathbf{V}} \|\mathbf{a}_i - \mathbf{V} \mathbf{r}^{(j)} - z\|_2^2.$$

4. Compute  $z^{(j)}$  via convex optimization to obtain  $z^{(j)} = \arg \min_z \|\mathbf{a}_i - \mathbf{V}^{(j)} \mathbf{r} - z\|_2^2 + \lambda_1 \|z\|_2^2$ .

**End**

**Output:** the design matrix  $\mathbf{V}^{(J)}$ , the sparse vector  $\mathbf{r}^{(J)}$ , and the noise term  $z^{(J)}$ .

---

#### D. Prediction error

Consequently, the proposed ML-based framework models the cellular traffic pattern as  $\tilde{\mathbf{d}}_i = \tilde{\mathbf{n}}_i + \tilde{\mathbf{a}}_i = \mathbf{w}^T \boldsymbol{\psi} + \mathbf{V} \mathbf{r} + z$ . Using such a model, the prediction error of the traffic demand for an unseen time  $t$ , with the actual load amount  $\mathbf{d}_i(t)$ , is given by:

$$\|\mathbf{d}_i(t) - \tilde{\mathbf{d}}_i(t)\| = \|(\mathbf{a}_i(t) + \tilde{\mathbf{n}}_i(t)) - (\tilde{\mathbf{n}}_i(t) + \tilde{\mathbf{a}}_i(t))\| = \|\mathbf{a}_i(t) - \tilde{\mathbf{a}}_i(t)\|. \quad (13)$$

Thus, the prediction error of model  $\tilde{\mathbf{d}}_i$  is determined only by the compressive sensing model  $\tilde{\mathbf{a}}_i$ . As a result, we derive an upper bound for the prediction error of the proposed iterative algorithm in Theorem 1 as follows.

**Theorem 1.** *The proposed cellular traffic model  $\tilde{\mathbf{d}}_i$  approximates the actual traffic load  $\mathbf{d}_i$  with a prediction error that is upper-bounded by*

$$\|\mathbf{d}_i - \tilde{\mathbf{d}}_i\| \leq \left| \frac{\eta_{\max}}{\eta_{\min}} \right| \sup \|z\|, \quad (14)$$

where  $\eta_{\max}$  and  $\eta_{\min}$  are the maximal and minimal non-zero singular value of the design matrix  $\mathbf{V}$ , respectively, and  $\sup \|z\|$  is the supremum of the norm of the noise term.

*Proof.* Here, we assume that the size of dataset  $\mathbf{d}_i$  for each BS  $i$  is large enough, such that both training data and test data are representative samples of the underlying traffic pattern. Thus, for an unseen time  $t$  with the actual amount  $\mathbf{d}_i(t)$ , there exist a reason vector  $\mathbf{r}^*$  such that

$\|\mathbf{a}_i - \mathbf{V}\mathbf{r}^* - z\| \leq o$ , where  $o$  is a negligible small positive value. Let  $\mathbf{r}$  be the output of the proposed learning approach in Algorithm 1. Then,

$$\|\mathbf{d}_i(t) - \tilde{\mathbf{d}}_i(t)\|^2 = \|\mathbf{a}_i(t) - \tilde{\mathbf{a}}_i(t)\|^2 \cong \|\mathbf{V}\mathbf{r}^* - \mathbf{V}\mathbf{r}\|^2 = \|\mathbf{V}(\mathbf{r}^* - \mathbf{r})\|^2, \quad (15)$$

According to [40],  $\|\mathbf{r}^* - \mathbf{r}\|^2 \leq \sup \|z\|^2 / \eta_{\min}^2$ . Thus, (15) can be re-written as

$$\|\mathbf{d}_i(t) - \tilde{\mathbf{d}}_i(t)\|^2 \cong \|\mathbf{V}(\mathbf{r}^* - \mathbf{r})\|^2 \leq \|\mathbf{V}\|^2 \|\mathbf{r}^* - \mathbf{r}\|^2 \leq \eta_{\max}^2 \frac{\sup \|z\|^2}{\eta_{\min}^2}, \quad (16)$$

which proves Theorem 1.  $\square$

Theorem 1 shows that the maximum prediction error of the proposed ML approach is determined by the singular values of design matrix  $\mathbf{V}$  and the power of noise term  $z$ . To improve the prediction accuracy, one can increase the weight  $\lambda_1$  of the noise term in (12) to lower the value of  $\sup \|z\|$ , and add constraints in the optimization iterations of Algorithm 1 to decrease the value of the singular values' ratio  $\left| \frac{\eta_{\max}}{\eta_{\min}} \right|$ . A lower value of  $\sup \|z\|$  implies that the proposed model is less noise-tolerant, and is more likely to treat the fluctuation in the traffic curve as a hotspot event, instead of a noise. On the other hand, a smaller ratio for the singular values  $\left| \frac{\eta_{\max}}{\eta_{\min}} \right|$  indicates that the excessive traffic loads caused by different congestion reasons will be more similar. In order to find the proper values of  $\lambda_1$  and  $\left| \frac{\eta_{\max}}{\eta_{\min}} \right|$ , parameter validation techniques [36] can be applied to avoid overfitting. Furthermore, Theorem 1 pinpoints the worst case of (7). That is, given the predicted traffic demand of BS  $i$  as  $\tilde{\mathbf{d}}_i(t) = \mathbf{w}^T \boldsymbol{\psi}(t) + \mathbf{V}(t)\mathbf{r}(t) + z$ , the utility of BS  $i$  is no less than a lower bound, where  $\max_{j \in \mathcal{J}, \Phi_i} U_{ij}(\phi_{ij}, \tilde{\mathbf{d}}_i(t)) \geq \beta B_{ij}(p_j) - u_i \tilde{\mathbf{d}}_i(t) - \delta \left| \frac{\eta_{\max}}{\eta_{\min}} \right| \sup \|z\|$ .

#### IV. CONTRACT MATCHING DESIGN FOR UAV ALLOCATION

##### A. Traffic offloading contract design

Given the predicted traffic demand  $\tilde{\mathbf{d}}_i(t)$ , each BS  $i \in \mathcal{I}$  can forecast possible network congestion, and request a UAV to offload wireless users, if needed, at the beginning of each time interval  $T$ . In order to find a qualified UAV with enough transmission power to offload traffic, each BS needs to carefully design a contract  $\phi_{ij} = (u_i, p_j)$  for each UAV  $j \in \mathcal{J}$ , and guarantee that each UAV  $j$  will truthfully reveal its communication capacity. To clearly demonstrate the relationship between  $u_i$  and  $p_j$  in the UAV's utility function, we divide by  $Tc_{ij}$  on both sides of (6) and rewrite the utility of UAV  $j$  as follows:

$$\tilde{R}_{ij}(u_i, p_j) = \theta_{ij} u_i - p_j, \quad (17)$$

where  $\theta_{ij} = \frac{\tilde{d}_i(t)}{Tc_{ij}} = \frac{\tilde{d}_i(t)p_{ij}^{\max}}{T\alpha_j}$  determines the sensitivity of  $\tilde{R}_{ij}$  to the increase of payment  $u_i$  and power  $p_j$ . Here, we define  $\theta_{ij}$  to be the *type* of UAV  $j$  with respect to BS  $i$ , and the range of  $\theta_{ij}$  is denoted by a continuous set  $\Theta = [\theta^{\min}, \theta^{\max}]$ , with  $\theta^{\min} \geq 0$ . Since each BS  $i \in \mathcal{I}$  does not have any knowledge on the maximum transmission power  $p_{ij}^{\max}$  and the energy cost efficiency  $\alpha_j$  of UAV  $j$ , the type  $\theta_{ij}$  is the private information of UAV  $j$ . Therefore, to employ a UAV with sufficient transmit power at a reasonable price, each BS  $i \in \mathcal{I}$  should design a set of contracts for all kinds of UAV's types  $\theta_{ij} \in \Theta$ , so as to guarantee that a UAV of any type will truthfully reveal its communication capacity.

We denote the contract set of BS  $i$  as  $\Phi_i(\Theta) = \{\phi_{ij}(\theta_{ij}) | \forall \theta_{ij} \in \Theta\} = \{(u_i(\theta_{ij}), p_j(\theta_{ij})) | \forall \theta_{ij} \in \Theta\}$ , where  $u_i(\theta_{ij})$  represents the payment that BS  $i$  pays to UAV  $j$  per bit of data, given that UAV  $j$  is of type  $\theta_{ij}$ , and  $p_j(\theta_{ij})$  is the transmit power that UAV  $j$  of type  $\theta_{ij}$  provides to serve BS  $i$ . In other words, the predicted data demand  $\tilde{d}_i(t)$  of BS  $i$ , the maximum transmit power  $p_{ij}^{\max}$ , and the energy cost efficiency  $\alpha_j$  of UAV  $j$  jointly determine the type  $\theta_{ij}$  of UAV  $j$  with respect to BS  $i$ , which further determines the values of the unit payment  $u_i(\theta_{ij})$  and transmit power  $p_j(\theta_{ij})$  of the contract  $\phi_{ij}$  between BS  $i$  and UAV  $j$ . To ensure that each UAV  $j \in \mathcal{J}$  only accepts the contract of its own type, based on contract theory [23], two constraints should be considered: individual rationality (IR) condition and incentive compatibility (IC) condition.

**Definition 1** (Individual Rationality). *A contract designed by BS  $i$  satisfies the IR constraint, if a UAV of any type  $\theta_{ij} \in \Theta$  will receive a non-negative payoff from BS  $i$  by accepting the contract item for type  $\theta_{ij}$ , i.e.  $\theta_{ij}u_i(\theta_{ij}) - p_j(\theta_{ij}) \geq 0$ .*

**Definition 2** (Incentive Compatibility). *A contract designed by BS  $i$  satisfies the IC constraint, if a UAV of type  $\theta_{ij}$  will get the highest utility from BS  $i$  by accepting the contract designed for its own type  $\theta_{ij}$ , compared with all the other types in  $\Theta$ , i.e.  $\theta_{ij}u_i(\theta_{ij}) - p_j(\theta_{ij}) \geq \theta_{ij}u_i(\theta'_{ij}) - p_j(\theta'_{ij}), \forall \theta'_{ij} \in \Theta$ .*

A contract satisfying both IC and IR conditions can guarantee that the UAV will accept and only accept the contract designed for its own type. Such contract is called a *feasible* contract. The inequalities in IC and IR conditions define the feasible range of the contract set  $\Phi_i$  of each BS  $i \in \mathcal{I}$ , in which each UAV  $j \in \mathcal{J}$  will accept the contract designed for its own type and truthfully provide the required transmit power to serve UAV users in the downlink. In order to design a feasible contract set  $\Phi_i$ , we need to analyze the sufficient and necessary conditions for

a contract that satisfies IC and IR conditions.

**Proposition 1.** *[Necessary Condition] For any  $\theta_{ij}, \theta'_{ij} \in \Theta$ , if  $\theta_{ij} > \theta'_{ij}$ , then  $u_i(\theta_{ij}) \geq u_i(\theta'_{ij})$  and  $p_j(\theta_{ij}) \geq p_j(\theta'_{ij})$ .*

*Proof.* See Appendix A. □

Proposition 1 shows that a UAV  $j$  with a higher type  $\theta_{ij}$  will receive a higher unit payment  $u_i$  from BS  $i$ , and, in return, it should provide a larger transmit power  $p_j$ . This conclusion will lead to the necessary and sufficient conditions of a feasible contract, as shown next.

**Theorem 2.** *[Necessary and Sufficient Condition] For a contract set  $\Phi = \{(u_i(\theta_{ij}), p_j(\theta_{ij})) | \forall \theta_{ij}\}$ , it is feasible if and only if all the following three conditions hold: (a)  $\frac{dp_j(\theta_{ij})}{d\theta_{ij}} \geq 0$  and  $\frac{du_i(\theta_{ij})}{d\theta_{ij}} \geq 0$ , (b)  $\theta^{min} u_i(\theta^{min}) - p_j(\theta^{min}) \geq 0$ , (c)  $\frac{dp_j(\theta_{ij})}{d\theta_{ij}} = \theta_{ij} \cdot \frac{du_i(\theta_{ij})}{d\theta_{ij}}$ .*

*Proof.* See Appendix B. □

For each BS  $i \in \mathcal{I}$ , a contract  $\Phi_i$  that satisfies Theorem 2 will guarantee that each UAV accepts only the contract designed for its own type, and provides the required transmit power to meet the aerial data demand of BS  $i$ . However, there exists an infinite number of solutions that satisfy Theorem 2. Thus, for each BS  $i \in \mathcal{I}$ , there are infinite ways to design a feasible contract set  $\Phi_i$ . To continue our discussion, we will take the simplest feasible solution of Theorem 2, where  $\frac{du_i(\theta_{ij})}{d\theta_{ij}} = \gamma > 0$  is a positive constant, and thus  $(u_i, p_j) = (\gamma\theta_{ij}, \gamma\theta_{ij}^2/2)$ . Here, the unit payment  $u_i$  of BS  $i$  linearly increases with UAV type  $\theta_{ij}$ , and the transmission power  $p_j$  of UAV  $j$  is a quadratic function of UAV type  $\theta_{ij}$ . Since such contract  $(u_i, p_j) = (\gamma\theta_{ij}, \gamma\theta_{ij}^2/2)$  is easy to implement, it is potential to be the best choice of the feasible contract for practical uses.

### B. Matching under the feasible contract

Consequently, given the feasible contract set  $\{(\gamma\theta_{ij}, \gamma\theta_{ij}^2/2) | \forall \theta_{ij}\}$ , the utility  $R_{ij}(\theta_{ij})$  of each UAV  $j$  with respect to each BS  $i$  and the utility  $U_{ij}(\theta_{ij})$  of each BS  $i$  with respect to each UAV  $j$  are jointly determined. Then, the last task is to optimally allocate UAVs to offload traffic from hotspot areas that maximizes the individual utility of each BS and UAV.

In order to properly model the interactions between multiple operators, the matching theory framework [29] can be used to study the optimal UAV allocation. A *matching game* is defined on two disjoint sets of players, here being, the BS set  $\mathcal{I}$  and the UAV set  $\mathcal{J}$ , where each player

$k$  of either set has an individual *preference list*  $\mathcal{P}_k$  that ranks the players from the other set, based on the utilities that players can provide to player  $k$ . The goal of each player is to form a pair with the most favorable player from the other set with a highest preference in  $\mathcal{P}$ . However, the matching relationship must be mutual. That is, to form a matching relationship, both players must mutually agree on the matching.

To construct a matching game, we first study the preference list of each UAV  $j \in \mathcal{J}$  towards BSs in  $\mathcal{I}$ . The utility of UAV  $j$  by serving BS  $i$  is

$$R_{ij} = u_i \tilde{d}_i(t) - T c_{ij} p_j = \gamma \theta_{ij} \tilde{d}_i(t) - \frac{\gamma}{2} T c_{ij} \theta_{ij}^2 = \frac{\gamma}{2} \theta_{ij} \tilde{d}_i(t). \quad (18)$$

Thus, the utility  $R_{ij}$  of UAV  $j$  will increase with the increase of UAV type  $\theta_{ij}$ . Given that  $\theta_{ij} = \frac{\tilde{d}_i(t) p_{ij}^{\max}}{T \alpha_j}$ , we finally have the expression of UAV  $j$ 's utility as  $R_{ij} = \frac{\gamma}{2 T \alpha_j} \tilde{d}_i^2(t) p_{ij}^{\max}$ . Therefore, in order to maximize the utility, each UAV  $j \in \mathcal{J}$  will either choose the closest BS  $i$  to maximize the value of  $p_{ij}^{\max}$ , or select the BS with the highest data demand  $\tilde{d}_i(t)$ . Consequently, each UAV  $j \in \mathcal{J}$  can form a preference list  $\mathcal{P}_j$ , based on the value of  $\tilde{d}_i^2(t) p_{ij}^{\max}$  associated with each BS  $i \in \mathcal{I}$ . Here, given  $i, k \in \mathcal{I}$  and  $i \neq k$ , we use the notation  $i \succ_j k$  to imply that player  $j$  prefers to accept the contract from BS  $i$  and provide it with aerial service, over BS  $k$ . Similarly, given that the utility of each BS  $i \in \mathcal{I}$  with respect to the UAV type is a concave function on  $[\theta_{\min}, \theta_{\max}]$ , using convex optimization techniques, each BS can form a preference list  $\mathcal{P}_i$  that ranks all UAV in  $\mathcal{J}$ , according to the utility that each UAV  $j$  can provide to BS  $i$ .

Note that, at each time, each BS can employ only one UAV for aerial cellular service, and each UAV only serves the area of a single BS. Using matching theory, the allocation result of UAVs can be defined by a one-to-one mapping relationship  $\eta$ , defined as follows. Here, without losing generality, we assume the number of UAVs  $|\mathcal{J}|$  is greater than the number of BSs  $|\mathcal{I}|$ .

**Definition 3.** In a matching game, given two disjoint finite sets of players  $\mathcal{I}$  and  $\mathcal{J}$ , a stable matching is defined as a one-to-one relationship  $\eta$  between  $\mathcal{I}$  and  $\mathcal{J}$ , where we have: (a).  $\forall i \in \mathcal{I}$ ,  $\eta(i) \in \mathcal{J}$ ; (b).  $\forall j \in \mathcal{J}$ ,  $\eta^{-1}(j) \in \mathcal{I} \cup \emptyset$ ; (c).  $\eta(i) = j$ , if and only if  $\eta^{-1}(j) = i$ ; (d).  $\forall i \in \mathcal{I}$  and  $j \in \mathcal{J}$ , there does not exist a pair  $(i, j)$  with  $\eta(i) \neq j$  and  $\eta^{-1}(j) \neq i$  such that  $j \succ_i \eta(i)$  and  $i \succ_j \eta^{-1}(j)$ .

Conditions (a)-(c) in Definition 3 require the matching  $\eta$  to be a one-to-one relationship between  $\mathcal{I}$  and  $\mathcal{J}$ , and requirement (d) guarantees the stability of the matching output, which is introduced to avoid the repeated selection. Note that, multiple BSs can compete for one UAV

---

**Algorithm 2** Deferred acceptance algorithm to find the stable matching  $\eta$ 


---

**Initialization:** Each BS  $i \in \mathcal{I}$  takes turns to broadcast its contract set  $\Phi_i$ , the predicted data demand  $\tilde{d}_i(t)$ , and the optimal service location  $\mathbf{x}_{ij}^*$  for the requested UAV. Each UAV  $j$  listens to the broadcast, calculate its type  $\theta_{ij}$  towards each BS  $i$ .

**Do**

1. Each UAV  $j$  with  $\eta^{-1}(j) = \emptyset$  sends its type  $\theta_{i^*j}$  to the BS  $i^*$  on the top of  $\mathcal{P}_i$ , where  $i^* = \arg \max_{i \in \mathcal{P}_j} \tilde{d}_i(t) \theta_{ij}$ .
2. Each BS  $i$  listens for the response. Let  $\mathcal{J}_i$  be the set of UAVs that responds to BS  $i$ .

**If**  $\mathcal{J}_i \neq \emptyset$  and  $\eta(i) = \emptyset$ , BS  $i$  confirms the matching relationship with UAV  $j^* = \arg \max_{j \in \mathcal{J}_i} U_{ij}$ , and denies the responses of all other UAVs;

**Elseif**  $\mathcal{J}_i \neq \emptyset$  and  $\eta(i) \in \mathcal{J}$ , BS  $i$  compares  $U_{i\eta(i)}$  with  $U_{ij^*}$ ,

**If**  $U_{i\eta(i)} \geq U_{ij^*}$ , BS  $i$  denies the responses of all UAVs, including UAV  $j^*$ .

**Else** BS  $i$  deletes the matching with  $\eta(i)$  and forms a new matching with UAV  $j^*$ .

**End**

**End**

3. If UAV  $j$  receives a denying or deleting message from a BS, it will delete this BS from its preference list  $\mathcal{P}_j$ .

**Until** Every UAV either forms a matching with some BS, or its preference list is empty.

---

that has the highest communication capability, and multiple UAVs can accept the contract from the same BS that provides the highest payment. In order to solve the conflict of being repeatedly selected, a stable matching  $\eta$  ensures that there does not exist two BSs  $i$  and  $i'$  with their matched UAVs  $j = \eta(i)$  and  $j' = \eta(i')$ , however, BS  $i$  prefers UAV  $j'$  to  $j$  and BS  $i'$  prefers UAV  $j$  to  $j'$ . In a word, to form a matching relationship, each BS and UAV must pairwise prefer each other over all the other possible pairs.

In order to find a stable matching  $\eta$ , an iterative and distributed method is proposed, based on the deferred acceptance algorithm, in Algorithm 2. Finally, as shown in [41], Algorithm 2 will converge to a stable matching  $\eta$ . Furthermore, it has been proven in [41] that the outcome of this algorithm provides UAV networks with the optimal utility among all stable matching results.

## V. SIMULATION RESULTS AND ANALYSIS

For our simulations, we consider a UAV cellular network operating at the 5 GHz frequency band to complement the ground LTE networks for downlink communications. For each UAV, the total available bandwidth is 20 MHz, the antenna gain is 5 dB, the average of mobility speed is 30 meter per second, and the propulsion power is 100 W [27]. The dataset in [30] is used for the modeling training, and validation of the ML framework, and 10-fold cross-validation is applied to evaluate the model performance. Once the ML output is determined, we choose an arbitrary

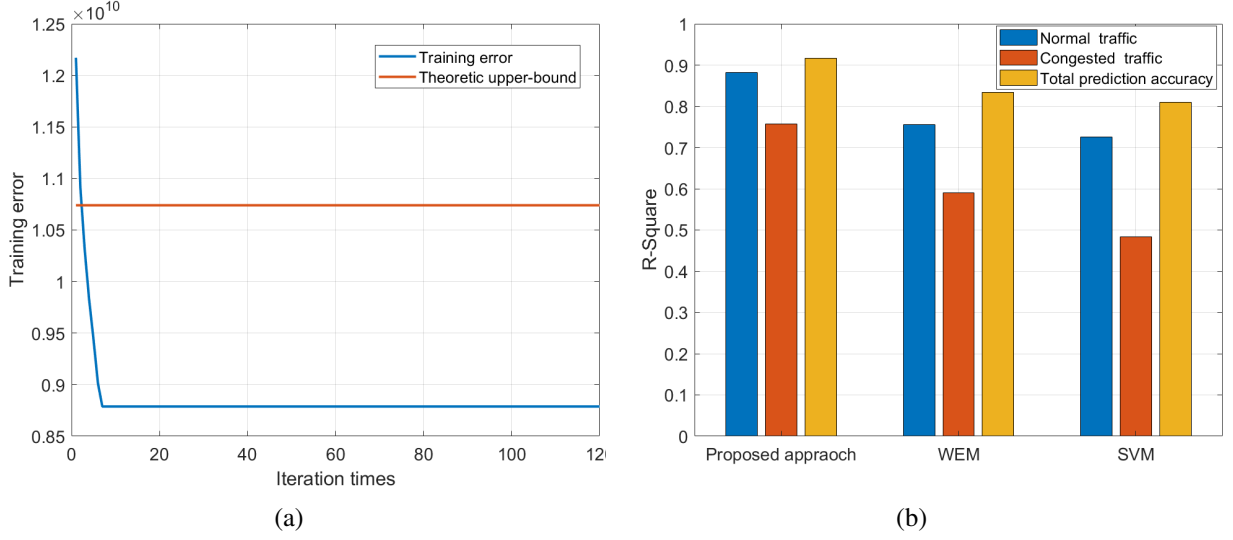


Fig. 5: (a) The training error of the proposed approach will decrease below the theoretic upper-bound. (b) The proposed approach significantly improves the prediction accuracy, defined by R-square, compared with the WEM and SVM methods.

time period, during which the number of congested BSs is 12, to evaluate the performance of the optimal UAV allocation. The utility parameters are set as  $\beta = 10e - 10$  and  $\gamma = 1e - 10$ .

Fig. 5a shows that, as the number of iterations increases, the training error of the proposed ML method decreases rapidly, and, on average, converges within ten iterations. Moreover, the sparse vector  $\mathbf{r}$  and the design matrix  $\mathbf{V}$  will converge to the best-correlated optimum, and the training error of the ML prediction algorithm will eventually drop below the theoretic upper-bound, which supports the conclusion of Theorem 1. In Fig. 5b, we compare the average prediction accuracy of the proposed approach with the Gaussian kernel SVM and WEM algorithms. Here, R-square, defined by  $R^2 = 1 - \sum_{t=1}^{t=m} (\tilde{a}(t) - a(t))^2 / \sum_{t=1}^{t=m} (a(t) - \bar{a}(t))^2$ , is used as the metric to evaluate the performance of each model. Fig. 5b first shows that the overall performance of the proposed ML approach yields an average accuracy gain of 10% and 13%, compared with WEM and SVM, respectively. To predict the cellular traffic demand under a normal network condition, all three models yield a high accuracy, greater than 0.8. However, when the downlink congestion occurs in the cellular network, the SVM and WEM methods fail to give accurate predictions on the traffic load, while the proposed approach presents a high accuracy of 0.76, which yields a significant performance gain of 28.3% and 56.6%, compared with WEM and SVM, respectively.

In Fig. 6, the utility functions  $R_{ij}(\theta)$  of four randomly-selected UAVs belonging to four different types: type 1, type 2, type 3, and type 4, based, respectively, on the values  $\theta_{ij} \in \{2701, 10674, 18817, 35800\}$ , are shown as the type of contract that each UAV chooses from a BS  $i$  changes. As shown in Fig. 6, the utility  $R_{ij}$  of each UAV  $j$  is a concave function

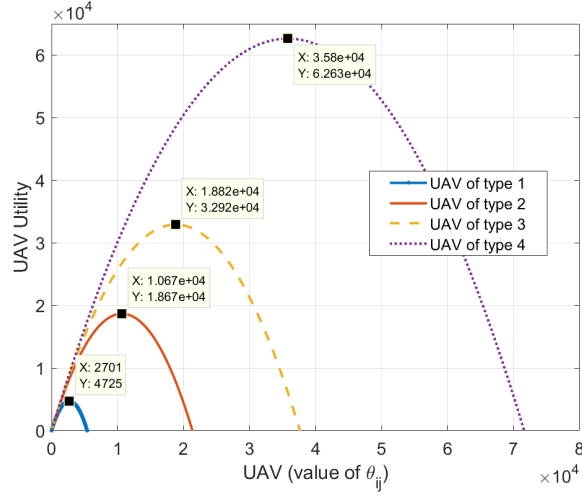


Fig. 6: The utility of each UAV is a concave function with respect to the contract type. The data cursors are placed at the maximum of each UAV's utility function.

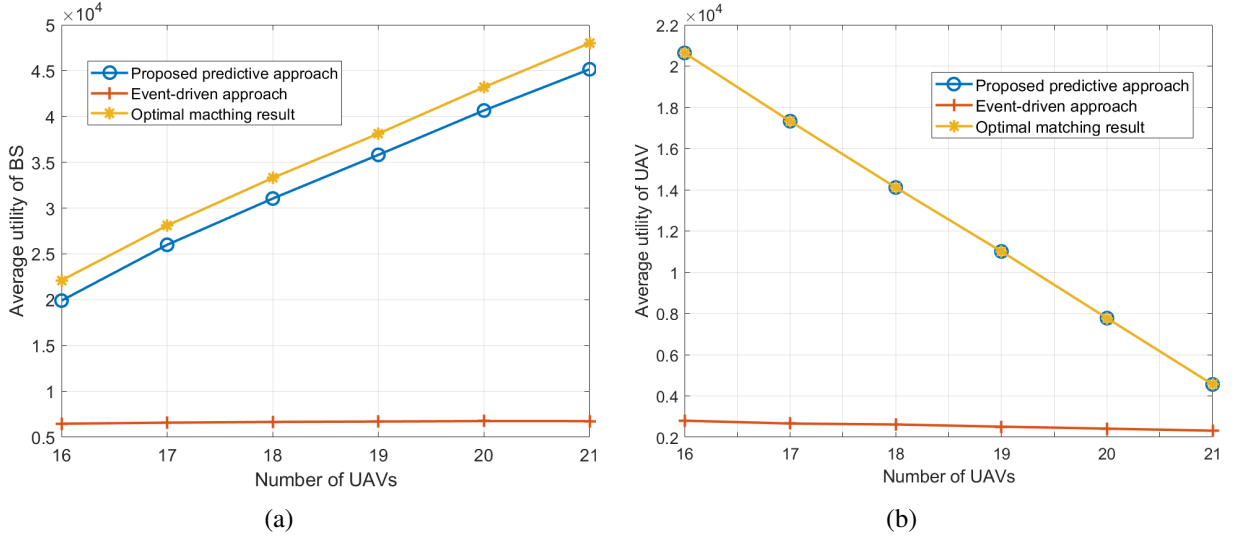


Fig. 7: When the number of requesting BSs is fixed, the average utility of BS networks increases and the average utility of UAV networks decreases, as the number of available UAVs increases.

of the contract type  $\theta$ , and the maximum of this utility is achieved when the contract type equals to the UAV type. Given the contract  $(\gamma\theta, \gamma\theta^2/2)$ , the utility achieved by UAV  $j$  when choosing any contract type  $\theta$  is given as  $R_{ij}(\theta) = \gamma\theta\tilde{d}_i(t) - \frac{1}{2}Tc_{ij}\gamma\theta^2 = \frac{\gamma\tilde{d}_i(t)}{2\theta_{ij}}[2\theta_{ij}\theta - \theta^2]$ . Thus,  $\theta_{ij} = \arg \max_{\theta} R_{ij}(\theta)$ . Therefore, to maximize its utility, each UAV  $j$  will always accept the contract designed for its own type. This result supports the conclusion of Theorem 2.

Fig. 7 shows the average per BS and per UAV utility, as the number of UAVs increases from 16 to 21, for three scenarios: the proposed predictive deployment of UAVs, an event-driven allocation, and the optimal exhaustive-search solution. In the proposed approach, each BS predicts the aerial demand using the proposed ML framework, and requests a UAV, via the contract

matching method, at the beginning of each period. However, in the event-driven allocation, each BS requests an aerial communication service only after the downlink congestion occurs, and the closest UAV will be deployed onto the service area of the requesting BS. The unit payment that each BS offers is constant, and, in return, each UAV will provide the downlink service to the best of its power ability. Furthermore, since the proposed approach jointly optimizes utilities for both BS and UAV operators in a distributed way, the output may be suboptimal. Here, we compare the utility of the proposed method with the highest utility, which each BS and UAV can receive among all stable allocation results of the contract matching problem. However, due to the conflicting interests, the optimal results for BSs and UAVs can not be achieved simultaneously in most cases.

Fig. 7a shows that, as the number of UAVs increases, the average utility per BS increases. Given that the number of requesting BSs is fixed, when more UAVs are available, each BS has more choices to employ a UAV with more desired communication power. From Fig. 7a, we can see that, compared with the event-driven baseline, the proposed approach yields a two-fold to six-fold improvement in the average per BS utility as the number of UAVs increases from 16 to 21. Note that, the utility of the event-driven approach is nearly constant. Since the event-driven approach does not consider the communication capability of a UAV when offloading traffic, the requested UAV usually provides a lower capacity than the real demand. Therefore, the event-driven approach is not able to efficiently improve the network performance. Furthermore, although the proposed approach does not yield the optimal result for the BS networks, the performance gap with the optimal solution is small. This gap is within the range of 6% to 10% as the number of UAVs varies.

Fig. 7b shows that, as the number of UAVs increases, the average per UAV utility in all scenarios will decrease. Given that the number of requesting BS UAVs is always 12, the number of employed UAVs is fixed. Therefore, as more UAVs are available, the average utility naturally decreases. Moreover, when more UAVs are available, each BS will prefer the cheaper UAV with enough communication power, thus the UAV network will have a lower average utility, and the improvement of the proposed approach, compared with the event-driven method, will decrease from six-fold to 60% as the number of UAV increases from 16 to 21. Fig. 7b further shows that the proposed distributed approach provides the UAV network with an optimal utility among all possible stable matching results.

## VI. CONCLUSION

In this paper, we have proposed a novel approach for predictive deployment of UAV aerial BSs to complement the ground cellular system in face of the prospective steep surge in cellular traffic. To enable the traffic prediction within each cellular network, a novel ML framework based on wavelet transform and compressive sensing has been proposed, which yields 10% and 13% gain in overall prediction accuracy, and 28.3% and 56.6% improvement of the demand prediction during hotspot events, compared with WEM and SVM methods, respectively. Given the predicted cellular traffic demand, we formulated the deployment of UAV BSs as a set of distributed optimization problems that jointly maximize the utility of each ground and UAV BS. In order to optimally solve the problem, a contract matching algorithm has been developed. Simulation results show that the proposed predictive deployment of UAVs yields a two-fold improvement in the average per BS utility and a 60% improvement in the average per UAV utility, compared with a baseline, event-driven allocation of UAVs to ground hotspot areas.

### APPENDIX A

#### PROOF OF PROPOSITION 1

We first use contradiction to prove the proposition that if  $\theta_{ij} > \theta'_{ij}$ , then  $u_i(\theta_{ij}) \geq u_i(\theta'_{ij})$ . Then, we prove that if  $u_i(\theta_{ij}) \geq u_i(\theta'_{ij})$ , then  $p_j(\theta_{ij}) \geq p_j(\theta'_{ij})$ . Suppose that there exists  $u_i(\theta_{ij}) < u_i(\theta'_{ij})$ , but  $\theta_{ij} > \theta'_{ij}$ . Then, we have

$$\theta_{ij}u_i(\theta'_{ij}) + \theta'_{ij}u_i(\theta_{ij}) > \theta_{ij}u_i(\theta_{ij}) + \theta'_{ij}u_i(\theta'_{ij}). \quad (19)$$

On the other hand, from IC condition, we have

$$\theta_{ij}u_i(\theta_{ij}) - p_j(\theta_{ij}) \geq \theta_{ij}u_i(\theta'_{ij}) - p_j(\theta'_{ij}), \quad (20)$$

$$\theta'_{ij}u_i(\theta'_{ij}) - p_j(\theta'_{ij}) \geq \theta'_{ij}u_i(\theta_{ij}) - p_j(\theta_{ij}). \quad (21)$$

By adding the inequation (20) and (21), we have

$$\theta_{ij}u_i(\theta_{ij}) + \theta'_{ij}u_i(\theta'_{ij}) \geq \theta_{ij}u_i(\theta'_{ij}) + \theta'_{ij}u_i(\theta_{ij}), \quad (22)$$

which contradicts to (19). This completes the first part of the proof.

Next, we prove that if  $u_i(\theta_{ij}) \geq u_i(\theta'_{ij})$ , then  $p_j(\theta_{ij}) \geq p_j(\theta'_{ij})$ . From the IC condition, we have

$$\theta'_{ij}u_i(\theta'_{ij}) - p_j(\theta'_{ij}) \geq \theta'_{ij}u_i(\theta_{ij}) - p_j(\theta_{ij}), \quad (23)$$

i.e.,  $p_j(\theta_{ij}) - p_j(\theta'_{ij}) \geq \theta'_{ij} (u_i(\theta_{ij}) - u_i(\theta'_{ij}))$ . Since  $u_i(\theta_{ij}) > u_i(\theta'_{ij})$ , we conclude

$$p_j(\theta_{ij}) - p_j(\theta'_{ij}) \geq \theta'_{ij} (u_i(\theta_{ij}) - u_i(\theta'_{ij})) \geq 0, \quad (24)$$

and thus  $p_j(\theta_{ij}) \geq p_j(\theta'_{ij})$ . This completes the proof.

## APPENDIX B

### PROOF OF THEOREM 2

For notational simplicity, we omit the subscript of variables  $u_i$ ,  $p_j$ ,  $\theta_{ij}$ , and denote them as  $u$ ,  $P$ ,  $\theta$ , respectively.

#### A. Proof for necessary conditions

Given the IR and IC conditions, we prove Theorem 2 in this section. First, as shown in Proposition 1, for any  $\theta, \theta' \in \Theta$ , once  $\theta > \theta'$ , then  $u(\theta) \geq u(\theta')$  and  $P(\theta) \geq P(\theta')$ , which proves condition (a) of Theorem 2 that  $\frac{dp_j}{d\theta_{ij}} \geq 0$  and  $\frac{du_i}{d\theta_{ij}} \geq 0$ . Then, the IR condition naturally support condition (b) of Theorem 2.

Then, we use the IC condition to prove condition (c). Let  $\Delta\theta = \theta' - \theta$ . According to the IC condition, for any  $\Delta\theta \in [\theta^{\min} - \theta^{\max}, 0) \cup (0, \theta^{\max} - \theta^{\min}]$ , we have

$$\theta \cdot u(\theta) - P(\theta) \geq \theta \cdot u(\theta + \Delta\theta) - P(\theta + \Delta\theta), \quad (25)$$

i.e.,

$$\theta \cdot [u(\theta) - u(\theta + \Delta\theta)] \geq P(\theta) - P(\theta + \Delta\theta). \quad (26)$$

If  $\Delta\theta > 0$ , then according to Proposition 1,  $u(\theta + \Delta\theta) \geq u(\theta)$  and  $P(\theta + \Delta\theta) \geq P(\theta)$ . Here, we exclude the situation where  $u(\theta + \Delta\theta) = u(\theta)$  and  $P(\theta + \Delta\theta) = P(\theta)$  in the following discussion of this proof, because condition (c) naturally holds under this situation. Therefore, for any  $\Delta\theta \in [\theta^{\min} - \theta^{\max}, 0)$ , we have

$$\theta \leq \frac{P(\theta + \Delta\theta) - P(\theta)}{u(\theta + \Delta\theta) - u(\theta)}. \quad (27)$$

If  $\Delta\theta < 0$ , then  $u(\theta + \Delta\theta) < u(\theta)$  and  $P(\theta + \Delta\theta) < P(\theta)$ . Thus, for any  $\Delta\theta \in (0, \theta^{\max} - \theta^{\min}]$ ,

$$\theta \geq \frac{P(\theta + \Delta\theta) - P(\theta)}{u(\theta + \Delta\theta) - u(\theta)}. \quad (28)$$

Consequently, by letting  $\Delta\theta \rightarrow 0$ , we have

$$\frac{dP}{d\theta} / \frac{du}{d\theta} = \lim_{\Delta\theta \rightarrow 0} \frac{P(\theta + \Delta\theta) - P(\theta)}{u(\theta + \Delta\theta) - u(\theta)} = \theta, \quad (29)$$

which proves condition (c) of Theorem 2.

### B. Proof for sufficient conditions

From Theorem 2, we will prove the IR and IC conditions in this section. First, we prove the IR condition. According to condition (b) of Theorem 2,  $\theta^{\min}$  satisfies the IR condition. Then, we prove that for any  $\theta \in (\theta^{\min}, \theta^{\max}]$ , the IR condition holds. From condition (c) of Theorem 2, we have the following inequalities,

$$\frac{P(\theta) - P(\theta^{\min})}{u(\theta) - u(\theta^{\min})} \leq \theta, \quad (30)$$

i.e.,

$$P(\theta^{\min}) \geq P(\theta) - \theta \cdot [u(\theta) - u(\theta^{\min})]. \quad (31)$$

From condition (b), we have

$$\theta^{\min} \cdot u(\theta^{\min}) \geq P(\theta^{\min}). \quad (32)$$

By combining (31) and (32), we have

$$\theta \cdot u(\theta) - P(\theta) \geq (\theta - \theta^{\min}) \cdot u(\theta^{\min}) \geq 0. \quad (33)$$

Thus, for any  $\theta \in \Theta$ , the IR condition holds.

In the end, we prove the IC condition. Let  $h = \theta \cdot u(\theta) - P(\theta) - [\theta \cdot u(\theta') - P(\theta')]$ . And we prove that  $h \geq 0$ . From condition (c), we have, if  $\theta' > \theta$ , then

$$\frac{P(\theta') - P(\theta)}{u(\theta') - u(\theta)} \geq \min\{\theta, \theta'\} = \theta. \quad (34)$$

i.e.,  $P(\theta') - P(\theta) \geq \theta \cdot [u(\theta') - u(\theta)]$ . Therefore,  $h = \theta \cdot [u(\theta) - u(\theta')] + P(\theta') - P(\theta) \geq 0$ . On the other hand, if  $\theta' < \theta$ , then

$$\frac{P(\theta) - P(\theta')}{u(\theta) - u(\theta')} \leq \max\{\theta, \theta'\} = \theta. \quad (35)$$

i.e.,  $P(\theta) - P(\theta') \leq \theta \cdot [u(\theta) - u(\theta')]$ . Therefore,  $h \geq 0$ . Consequently, the IC condition holds for any  $\theta, \theta' \in \Theta$ .

## REFERENCES

- [1] Q. Zhang, M. Mozaffari, W. Saad, M. Bennis, and M. Debbah, "Machine learning for predictive on-demand deployment of UAVs for wireless communications," in *Proc. of IEEE Global Communications Conference (GLOBECOM)*, Abu Dhabi, UAE, Dec 2018, pp. 1–6.
- [2] M. Mozaffari, W. Saad, M. Bennis, and M. Debbah, "Mobile unmanned aerial vehicles (UAVs) for energy-efficient internet of things communications," *IEEE Transactions on Wireless Communications*, vol. 16, no. 11, pp. 7574–7589, Sep 2017.

- [3] R. I. Bor-Yaliniz, A. El-Keyi, and H. Yanikomeroglu, "Efficient 3-D placement of an aerial base station in next generation cellular networks," in *Proc. of IEEE International Conference on Communications (ICC)*, Kuala Lumpur, Malaysia, May 2016, pp. 1–5.
- [4] X. Zhang and L. Duan, "Fast deployment of UAV networks for optimal wireless coverage," *IEEE Transactions on Mobile Computing*, May 2018.
- [5] W. Khawaja, I. Guvenc, D. Matolak, U.-C. Fiebig, and N. Schneckenberger, "A survey of air-to-ground propagation channel modeling for unmanned aerial vehicles," *arXiv preprint arXiv:1801.01656*, 2018.
- [6] M. Mozaffari, W. Saad, M. Bennis, Y.-H. Nam, and M. Debbah, "A tutorial on UAVs for wireless networks: Applications, challenges, and open problems," *arXiv preprint arXiv:1803.00680*, 2018.
- [7] M. Mozaffari, W. Saad, M. Bennis, and M. Debbah, "Unmanned aerial vehicle with underlaid device-to-device communications: Performance and tradeoffs," *IEEE Transactions on Wireless Communications*, vol. 15, no. 6, pp. 3949–3963, Feb 2016.
- [8] M. Chen, U. Challita, W. Saad, C. Yin, and M. Debbah, "Machine learning for wireless networks with artificial intelligence: A tutorial on neural networks," *arXiv preprint arXiv:1710.02913*, 2017.
- [9] Z. Hu, Z. Zheng, L. Song, T. Wang, and X. Li, "UAV offloading: Spectrum trading contract design for UAV assisted cellular networks," *IEEE Transactions on Wireless Communications*, vol. 17, no. 9, pp. 6093–6107, July 2018.
- [10] M. Mozaffari, W. Saad, M. Bennis, and M. Debbah, "Optimal transport theory for power-efficient deployment of unmanned aerial vehicles," in *Proc. of IEEE International Conference on Communications (ICC)*, Kuala Lumpur, Malaysia, May 2016, pp. 1–6.
- [11] E. Kalantari, H. Yanikomeroglu, and A. Yongacoglu, "On the number and 3D placement of drone base stations in wireless cellular networks," in *Proc. of IEEE 84th Vehicular Technology Conference (VTC-Fall)*, Montreal, QC, Canada, Sept 2016, pp. 1–6.
- [12] J. Lyu, Y. Zeng, and R. Zhang, "UAV-aided offloading for cellular hotspot," *IEEE Transactions on Wireless Communications*, vol. 17, no. 6, pp. 3988–4001, Mar 2018.
- [13] V. Sharma, M. Bennis, and R. Kumar, "UAV-assisted heterogeneous networks for capacity enhancement," *IEEE Communications Letters*, vol. 20, no. 6, pp. 1207–1210, Apr 2016.
- [14] J. Lyu, Y. Zeng, and R. Zhang, "Spectrum sharing and cyclical multiple access in UAV-aided cellular offloading," in *Proc. of IEEE Global Communications Conference (GLOBECOM)*, Singapore, Dec 2017, pp. 1–6.
- [15] F. Cheng, S. Zhang, Z. Li, Y. Chen, N. Zhao, R. Yu, and V. C. Leung, "UAV trajectory optimization for data offloading at the edge of multiple cells," *IEEE Transactions on Vehicular Technology*, vol. 67, no. 7, pp. 6732 – 6736, Mar 2018.
- [16] S. Sharafeddine and R. Islambouli, "On-demand deployment of multiple aerial base stations for traffic offloading and network recovery," *arXiv preprint arXiv:1807.02009*, 2018.
- [17] R. Li, Z. Zhao, J. Zheng, C. Mei, Y. Cai, and H. Zhang, "The learning and prediction of application-level traffic data in cellular networks," *IEEE Transactions on Wireless Communications*, vol. 16, no. 6, pp. 3899–3912, Mar 2017.
- [18] C. Yu, Y. Liu, D. Yao, L. T. Yang, H. Jin, H. Chen, and Q. Ding, "Modeling user activity patterns for next-place prediction," *IEEE Systems Journal*, vol. 11, no. 2, pp. 1060–1071, July 2017.
- [19] P. Valente Klaine, M. A. Imran, O. Onireti, and R. D. Souza, "A survey of machine learning techniques applied to self organizing cellular networks," *IEEE Communications Surveys and Tutorials*, vol. 19, no. 4, pp. 2392–2431, July 2017.
- [20] M. Chen, W. Saad, and C. Yin, "Liquid state machine learning for resource and cache management in LTE-U unmanned aerial vehicle (UAV) networks," *arXiv preprint arXiv:1801.09339*, 2018.
- [21] J. Chen, U. Yatnalli, and D. Gesbert, "Learning radio maps for UAV-aided wireless networks: A segmented regression approach," in *Proc. of IEEE International Conference on Communications (ICC)*, Paris, France, May 2017, pp. 1–6.

- [22] R. Amorim, J. Wigard, H. Nguyen, I. Z. Kovacs, and P. Mogensen, "Machine-learning identification of airborne UAV-UEs based on LTE radio measurements," in *Proc. of IEEE Globecom Workshops (GC Wkshps)*, Singapore, Jan 2017, pp. 1–6.
- [23] P. Bolton and M. Dewatripont, *Contract theory*. MIT press, 2005.
- [24] Y. Shi, R. Enami, J. Wensowitch, and J. Camp, "UABeam: UAV-Based beamforming system analysis with in-field air-to-ground channels," in *Proc. of IEEE International Conference on Sensing, Communication, and Networking (SECON)*, Hong Kong, China, June 2018, pp. 1–9.
- [25] A. Al-Hourani, S. Kandeepan, and A. Jamalipour, "Modeling air-to-ground path loss for low altitude platforms in urban environments," in *Proc. of IEEE Global Communications Conference (GLOBECOM)*, Austin, TX, USA, Dec 2014, pp. 2898–2904.
- [26] F. Lagum, I. Bor-Yaliniz, and H. Yanikomeroglu, "Strategic densification with uav-bss in cellular networks," *IEEE Wireless Communications Letters*, vol. 7, no. 3, pp. 384–387, June 2018.
- [27] Y. Zeng, J. Xu, and R. Zhang, "Energy minimization for wireless communication with rotary-wing uav," *arXiv preprint arXiv:1804.02238*, Apr 2018.
- [28] A. Nedic and A. Ozdaglar, "Distributed subgradient methods for multi-agent optimization," *IEEE Transactions on Automatic Control*, vol. 54, no. 1, pp. 48–61, Jan 2009.
- [29] Y. Gu, W. Saad, M. Bennis, M. Debbah, and Z. Han, "Matching theory for future wireless networks: fundamentals and applications," *IEEE Communications Magazine*, vol. 53, no. 5, pp. 52–59, May 2015.
- [30] "City cellular traffic map," <https://github.com/caesar0301/city-cellular-traffic-map>, accessed: 2016-10-05.
- [31] J. Gao, G. Hu, X. Yao, and R. K. Chang, "Anomaly detection of network traffic based on wavelet packet," in *Proc. of IEEE Asia-Pacific Conference on Communications*, Busan, South Korea, Aug 2006, pp. 1–5.
- [32] Y. Zang, F. Ni, Z. Feng, S. Cui, and Z. Ding, "Wavelet transform processing for cellular traffic prediction in machine learning networks," in *Proc. of China Summit and International Conference on Signal and Information Processing (ChinaSIP)*, Chengdu, China, July 2015, pp. 458–462.
- [33] D. Kwon, K. Ko, M. Vannucci, A. N. Reddy, and S. Kim, "Wavelet methods for the detection of anomalies and their application to network traffic analysis," *Quality and Reliability Engineering International*, vol. 22, no. 8, pp. 953–969, May 2006.
- [34] R. G. Garroppo and S. Niccolini, "Anomaly detection mechanisms to find social events using cellular traffic data," *Computer Communications*, vol. 116, pp. 240–252, Jan 2018.
- [35] X. Wang, Z. Zhou, Z. Yang, Y. Liu, and C. Peng, "Spatio-temporal analysis and prediction of cellular traffic in metropolis," in *Proc. of IEEE International Conference on Network Protocols (ICNP)*, Toronto, Canada, Oct 2017, pp. 1–10.
- [36] M. B. Christopher, *Pattern recognition and machine learning*. Springer-Verlag New York, 2016.
- [37] R. G. Baraniuk, "Compressive sensing [lecture notes]," *IEEE Signal Processing Magazine*, vol. 24, no. 4, pp. 118–121, July 2007.
- [38] B. Efron, T. Hastie, I. Johnstone, R. Tibshirani *et al.*, "Least angle regression," *The Annals of statistics*, vol. 32, no. 2, pp. 407–499, 2004.
- [39] J. Mairal, F. Bach, J. Ponce, and G. Sapiro, "Online learning for matrix factorization and sparse coding," *Journal of Machine Learning Research*, vol. 11, pp. 19–60, Jan 2010.
- [40] D. L. Donoho, M. Elad, and V. N. Temlyakov, "Stable recovery of sparse overcomplete representations in the presence of noise," *IEEE Transactions on Information Theory*, vol. 52, no. 1, pp. 6–18, Dec 2006.
- [41] A. E. Roth, "Deferred acceptance algorithms: History, theory, practice, and open questions," *International Journal of Game Theory*, vol. 36, no. 3-4, pp. 537–569, 2008.